ORIGINAL ARTICLE

Determination of optimal ^{68} Ga-PSMA PET/CT imaging time in prostate cancers by total-body dynamic PET/CT

Jun Wen[1] · Yinjie Zhu[2] · Lianghua Li[1] · Jianjun Liu[1] · Yumei Chen[1] · Ruohua Chen[1]

Abstract

Background ^{68} Ga-PSMA PET/CT has been widely used in patients with prostate cancer. Due to the limited axial field of view of conventional PET scanners, whole-body dynamic ^{68} Ga-PSMA PET/CT has not been performed. We investigated the time-activity curves (TACs) of prostate cancer pathological lesions and physiologic bladder activity to determine the optimal ^{68} Ga-PSMA PET/CT imaging time by total-body (TB) PET/CT.

Methods Dynamic TB-PET performed on 11 patients with prostate cancer was analyzed. TACs were obtained by drawing regions of interest in normal organs and pathological lesions (primary prostate lesions and lymph nodes and bone metastases). We evaluated the ^{68} Ga-PSMA uptake pattern of normal organs, urinary bladder, and pathological lesions.

Results The urinary bladder TAC increased slowly between 180 and 330 s post-injection and then rapidly between 5.5 and 60.0 min post-injection. The pathological lesion uptake increased rapidly during the first 5 min post-injection and then slowly through the remaining 55 min. Six minutes post-injection was the optimal time with the highest pathological lesion SUV_{mean} values still higher than the urinary bladder activity value. However, these prostate lesion, lymph node metastasis, and bone metastasis SUV_{mean} values were one-third, one-half, and one-half the corresponding values 60 min post-injection, suggesting that early imaging might miss low PSMA uptake lesions. A minimum of 35 min post-injection was required for the pathological lesions to have SUV_{mean} values similar to the corresponding values at 60 min post-injection (all $P > 0.05$), even though the pathological lesion SUV_{mean} values showed a continuous upward trend through the 60 min.

Conclusions Combining early dynamic ^{68} Ga-PSMA PET (75–360 s) and conventional static imaging 60 min post-injection could avoid the urinary bladder activity interference to better detect pathological lesions and lesions with relatively low PSMA uptake. The pathological lesion SUV_{mean} values at 35–59 min and 60 min post-injection were similar, so ^{68} Ga-PSMA PET imaging could also be made at 35–59 min post-injection.

Keywords Dynamic imaging · Prostate-specific membrane antigen (PSMA) · Prostate cancer · Early imaging

---

Jun Wen, Yinjie Zhu and Lianghua Li contributed equally to this article.

This article is part of the Topical Collection on Oncology—Genitourinary

✉ Jianjun Liu
nuclearj@163.com

✉ Yumei Chen
15921888559@163.com

✉ Ruohua Chen
crh19870405@163.com

1 Department of Nuclear Medicine, Ren Ji Hospital, School of Medicine, Shanghai Jiao Tong University, 160 Pujian Road, Shanghai 200127, China

2 Department of Urology, Ren Ji Hospital, School of Medicine, Shanghai Jiao Tong University, Shanghai, China

Introduction

Prostate cancer imaging sensitivity has significantly improved since ^{68} Ga-PSMA PET/CT was introduced in 2012 [1]. Various studies showed that the detection rate with ^{68} Ga-PSMA PET/CT was higher than that with conventional imaging approaches [1, 2]. Although no standard protocol has been defined, static ^{68} Ga-PSMA PET/CT 60 min post-tracer injection (p.i.) is recommended in clinical routine [3]. However, intense physiological urinary bladder uptake is already present at this point [3, 4]. Consequently, small lesions such as local recurrences or lymph node metastases adjacent to the urinary bladder might be overlooked. To improve positive lesion detection rates near the urinary bladder, researchers have reduced urinary bladder activity

by administering diuretics or voiding the bladder before PET imaging [5]. However, these methods did not reduce the urinary bladder activity sufficiently.

To determine whether dynamic [68] Ga-PSMA PET in patients with prostate cancer could avoid the effect of urinary bladder activity when evaluating the lesions, Virgolini et al. [6] performed early dynamic [68] Ga-PSMA PET imaging during the first 8 min p.i., showing that it could differentiate pathological tracer uptake from physiological bladder activity. However, due to the limited axial field of view (AFOV) of conventional PET scanners (15–30 cm), dynamic imaging was limited to the pelvic region, and only early imaging was applied. Furthermore, fast tracer dynamic capturing was not feasible in these conventional PET studies because of the relatively low sensitivity and signal-to-noise ratio. Dynamic images were acquired in these studies at a rate of 60 s per frame. However, changes in pathological [68] Ga-PSMA tracer uptake by the prostate cancer lesions and physiologic bladder activity occur very fast during the first few minutes p.i., so 60 s per frame might be too slow to observe real-time changes in [68] Ga-PSMA uptake.

The first total-body (TB) PET/CT (uEXPLORER, United Imaging Healthcare) ushered in 2019 the era of TB-PET with an AFOV of 194 cm [7]. This step allowed TB coverage with an overall > 40-fold gain in effective sensitivity and a > sixfold increase in the signal-to-noise ratio [8–10]. The improved sensitivity allowed for more precise dynamic imaging of the physiological uptake of all organs during ^{18}F-FDG PET/CT [11]. While TB dynamic analysis on ^{18}F-FDG PET/CT has been reported by Shi et al. [11], there are no reports of TB dynamic imaging with other tracers so far.

Therefore, our study aimed to analyze the TACs of normal organs, urinary bladder activity, and pathological lesions and determine the optimal prostate cancer [68] Ga-PSMA PET/CT imaging time by TB PET/CT.

Materials and methods

Participants

Eleven consecutive patients with prostate cancer referred to Renji Hospital for [68] Ga-PSMA PET/CT from December 2020 to July 2021 were retrospectively analyzed. [68] Ga-PSMA PET/CT was performed in eight patients for primary staging after prostate cancer confirmation by biopsy, and in three patients for evaluation after radical prostatectomy. The patient characteristics are shown in Table 1. The study followed the principles of the Declaration of Helsinki and its subsequent amendments. This retrospective study has been approved by the ethics committee of Renji Hospital, and the informed consent was waived.

Table 1 Patient characteristics

Patients (n)	11
Preoperative staging	8
Postoperative evaluation	3
Age (years)	69 (63–71)
Injected dose (Mbq)	145 (132–163)
PSA (ng/ml)	20.8 (0.5–74.0)
Gleason score	8 (7–9)
Number of pathological lesions	41
Number of primary prostate lesions	8
Number of lymph node metastases	17
Number of bone metastases	16

Configuration of the TB-PET/CT

The TB-PET/CT (uEXPLORER, United Imaging Healthcare) has a transaxial FOV of 68.6 cm and a long AFOV of 194 cm. Lutetium-yttrium oxyorthosilicate scintillator crystals with size of $18 \times 2.76 \times 2.76$ mm^3 are used for the PET detector, which are arrayed in detector blocks of 7×6 with a pitch of 2.85 mm. Every array is read out to 6×4.6mm^2 silicon photomultipliers. The PET scanner has eight axial ring units with an axial length, inter-unit gap, and inner-ring diameter of 24 cm, 2.6 mm, and 78.6 cm, respectively. Every ring consists of 24 detector modules and every module consists of 14×5 detector blocks. The time-of-flight technique is used with energy resolution and time of approximately 11.7% and 430 ps, respectively. The spatial resolution in the center of the FOV is 2.9 mm. The maximal acceptance angle of the detector is 57°. A 160-slice, 80-row CT scanner is integrated into this system.

Radiopharmaceutical

The PSMA ligand, [68] Ga-PSMA-11, was synthesized by Renji nuclear medicine laboratory. The laboratory has good-quality manufacturing practice and used a procedure as previously described [12]. The radiochemical purity of the final product was > 90%, as analyzed by thin-layer chromatography and reversed-phase high-performance liquid chromatography.

Dynamic data acquisition and reconstruction

Before [68] Ga-PSMA PET/CT scanning, weight and height were measured. The injected dose of [68] Ga-PSMA was 1.85 MBq/kg according to the guideline of the European Association of Nuclear Medicine for [68] Ga-PSMA PET/CT examinations [3]. Low-dose CT was used for attenuation correction. Then, 0–60 min dynamic PET was started

Fig. 1 Whole-body dynamic ^{68}Ga-PSMA PET/CT plan
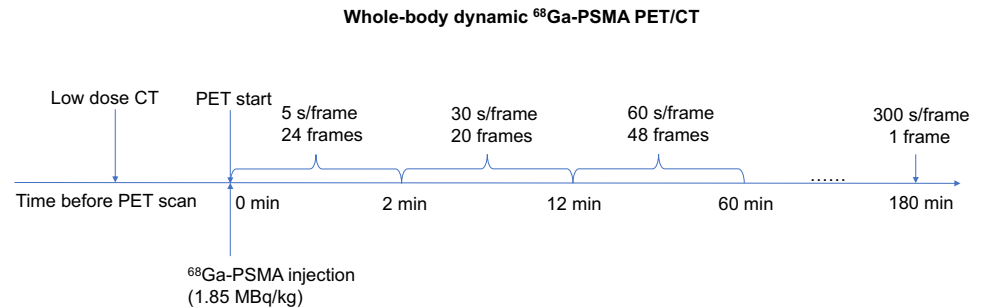
simultaneously with a bolus injection of ^{68}Ga-PSMA into a vein near the ankle. Though ^{68}Ga-PSMA is often injected in the hands, the physiological uptake of hand vein will affect the observation of pelvic lesions if patients drop their hands, especially in the early stage of dynamic imaging. If the patient put their hands over the heads, it is not easy for patients to stay still for 60 min. So the ^{68}Ga-PSMA was injected in the feet in our study.

The images were reconstructed by the list-mode ordered subsets expectation maximization algorithm incorporating TOF and point spread function modeling [10]. For dynamic analysis, the images were divided into 92 + 1 frames: every 5 s a frame for the initial 2 min (24 × 5 s), every 30 s min a frame (20 × 30 s) within 2–12 min p.i., and every 1 min a frame thereafter to 60 min (48 × 60 s). ^{68}Ga-PSMA PET/CT was also conducted from time 180 to 185 min p.i. (Fig. 1).

Generation of the time-activity curves

The frame-divided images were transferred to a workstation (uWSMI R001; United Imaging Healthcare)

for dynamic analysis. The largest regions of interest (ROIs) were drawn within the boundaries of normal organs and pathological lesions. Normal organs included the ascending aorta, cerebral cortex, lung (right), liver, spleen, pancreas, bone (lumbar), muscle (gluteus maximus), parotid gland (right), submandibular gland (right), and kidney (right). Pathological lesions included primary prostate lesions and metastases to the lymph nodes and bone. The average radioactivity (kBq/mL) (SUVmean) within each ROI at each frame was used for the TACs.

Statistical analysis

Data are presented as mean ± standard deviation (SD) or mean (range). All hypothesis tests were two-sided with a significance level of 0.05. All statistical analyses were performed using SPSS Statistics for Windows, Version 13.0 (SPSS Inc., Chicago, IL, USA). Figures 3, 4, and 6 were generated by GraphPad Prism 6 (GraphPad Software Inc., San Diego, CA, USA).
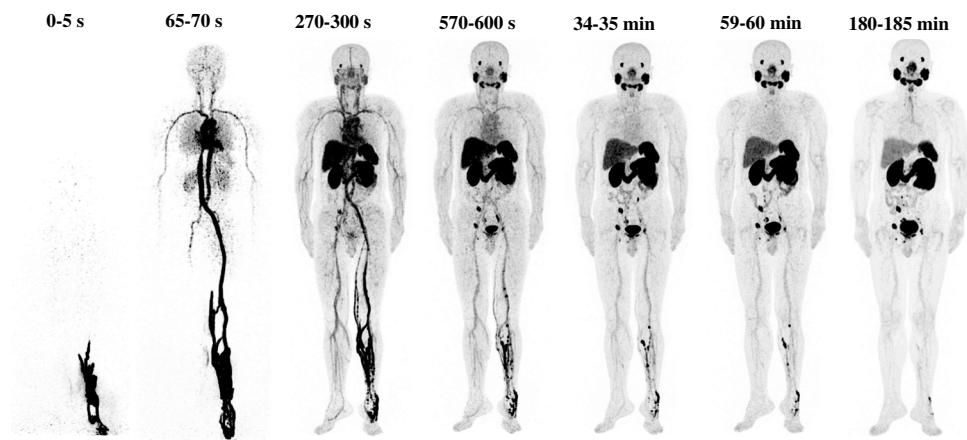

Fig. 2 Maximum intensity projection of selected dynamic reconstructed images of a 63-year-old patient with prostate cancer and lymph node and bone metastases. Frame 1 (0–5 s): Starting the ^{68}Ga-PSMA injection. Frame 14 (65–70 s): The ascending aorta reached its highest SUV_{mean}. Frame 30 (270–300 s): Pathological lesions (prostate lesions and bone metastases) were visualized on the maximum intensity projection (MIP) while the urinary bladder activity

was not. Frame 40 (570–600 s): The pathological lesions (prostate lesions and bone metastases) SUV_{mean} exceeded the urinary bladder activity. Frame 67 (34–35 min): The last time ^{68}Ga-PSMA PET/CT conducted before the 60 min p.i. scan. Frame 92 (59–60 min): This ^{68}Ga-PSMA PET/CT scan was similar to the conventional static 60 min p.i. scan. Frame 93 (180–185 min): Delayed ^{68}Ga-PSMA PET/CT image

Results

Maximum intensity projection of selected dynamic reconstructed images

All dynamic reconstructed images with 92 frames are shown in Supplementary information. Representative PET images acquired at 0–5 s (frame 1), 75–80 s (frame 14), 270–300 s (frame 30), 570–600 s (frame 40), 34–35 min (frame 67), 59–60 min (frame 92), and 180–185 min (frame 93) are shown in Fig. 2.

PET/CT studies 60 min p.i.

The patient characteristics are shown in Table 1. Among the 11 patients, nine patients (eight for evaluating primary staging, and 1 for evaluation after radical prostatectomy) showed at least one lesion with pathological uptake on TB ^{68}Ga-PSMA PET/CT scans 60 min p.i., totaling 41 lesions. Two patients for evaluation after radical prostatectomy did not have any pathological uptake. Of these 41 lesions, 8 were the primary prostate lesions, 17 in the lymph nodes, and 16 in the bones. The primary prostate lesions were all verified histologically with biopsy. Fifteen lymph nodes and 14 bones with pathological uptake were confirmed with conventional imaging or follow-up PET/CT. Two lymph nodes and 2 bones with pathological uptake could not be verified.

TAC of normal organs

The TACs of normal organs are shown in Fig. 3 and Table 2. The uptake in the ascending aorta, cerebral cortex, and lung rapidly increased and rapidly decreased; the times to reach the highest SUV_{mean} in the ascending aorta, cerebral cortex, and lung were (67 ± 22) s, (82 ± 27) s, and (72 ± 32) s, respectively. The uptake in the liver, spleen, pancreas, bone, and muscle rapidly increased and slowly decreased; the times to reach the highest SUV_{mean} in the liver, spleen, pancreas, bone, and muscle were (583 ± 365) s, (696 ± 480) s, and (100 ± 29) s, (190 ± 135) s, and (433 ± 265) s, respectively. The uptake in the parotid gland, submandibular gland, and kidney gradually increased.

Urinary bladder activity and pathological lesions' TACs

The urinary bladder activity and pathological lesions' TACs are shown in Fig. 4 and Table 3. The urinary bladder activity, assessed in all 11 patients, was not detectable within the first 3 min (Fig. 4A), showed flat and slow ascent with a SUV_{mean} of 0.6 ± 0.3 5.5 min p.i., and rapidly increased after that until the end of the dynamic study (SUV_{mean} at 60 min p.i., 62.4 ± 31.0).
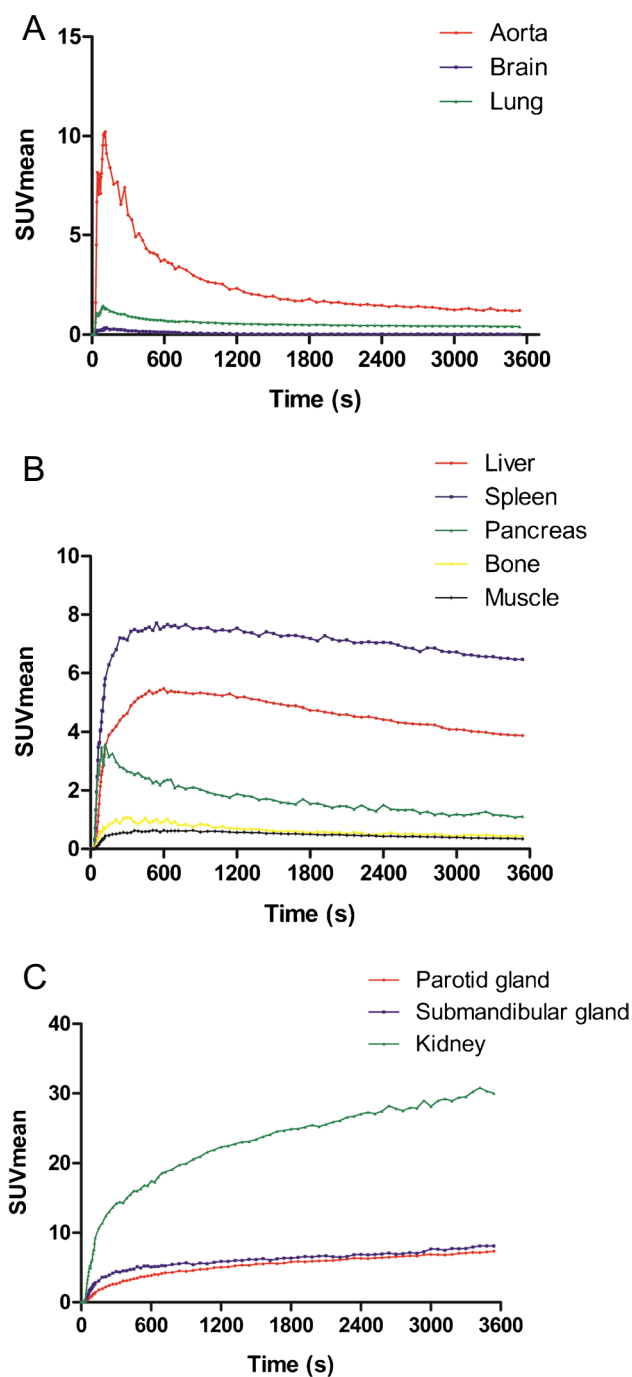

Fig. 3 Time-activity curves of normal organs. **A** The ascending aorta, cerebral cortex, and lung uptake rapidly increased and rapidly decreased. **B** Liver, spleen, pancreas, bone, and muscle uptake rapidly increased and slowly decreased. **C** Parotid gland, submandibular gland, and kidney uptake gradually increased

Tracer uptake by the primary prostate lesions started very early, increased rapidly during the first 5 min, and increased more slowly until the end of the dynamic study (Fig. 4B). The prostate lesion SUV_{mean} was higher than that of the urinary bladder activity between 70 and 420 s p.i.

Table 2 Uptake pattern of normal organs

| Uptake pattern	Normal organs	The time to reach the highest SUV_{mean}	The highest SUV_{mean}	The SUV_{mean} at 60 min p.i
Rapid increasing and rapid decreasing	Ascending aorta	(67 ± 22) s	15.9 ± 7.8	1.2 ± 0.3
	Cerebral cortex	(82 ± 27) s	0.5 ± 0.3	0.02 ± 0.01
Rapid increasing and slow decreasing	Lung	(72 ± 32) s	2.2 ± 1.4	0.4 ± 0.1
	Liver	(583 ± 365) s	5.9 ± 1.7	3.9 ± 1.4
	Spleen	(696 ± 480) s	8.6 ± 2.6	6.5 ± 2.5
	Pancreas	(100 ± 29) s	4.5 ± 2.0	1.1 ± 0.4
	Bone	(190 ± 135) s	1.4 ± 0.9	0.4 ± 0.2
	Muscle	(433 ± 265) s	0.7 ± 0.2	0.3 ± 0.1
Gradually increasing	Parotid gland	3600 s	7.4 ± 2.7	7.4 ± 2.7
	Submandibular gland	3600 s	8.1 ± 3.6	8.1 ± 3.6
	Kidney	3600 s	30.0 ± 15.6	30.0 ± 15.6
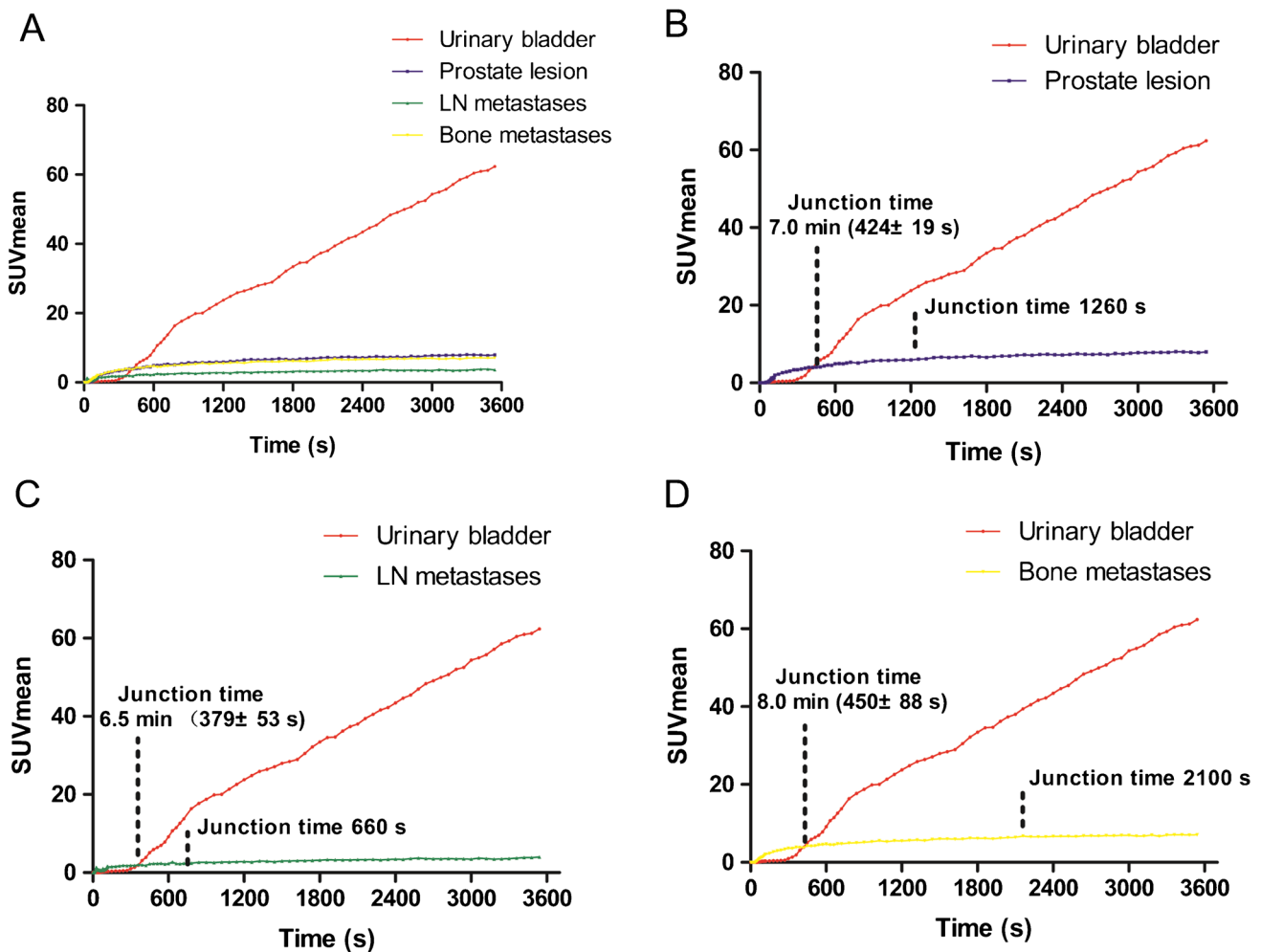
Fig. 4 Time-activity curves of the urinary bladder activity and pathological lesions. **A** A comparison of the pathological lesions (prostate lesions, lymph node metastases, and bone metastases) and urinary bladder activity curves. **B** Primary prostate lesions' tracer uptake started very early (mean, 86 s; range, 75–100 s). The prostate lesions and urinary bladder activity had equal SUV_{mean} (junction time) 7 min $(424 \pm 19$ s) post-tracer injection (p.i.), and 21 min p.i. was the minimum time when their SUV_{mean} value was similar to that at 60 min p.i.

C Lymph node metastases' tracer uptake started very early (mean, 35 s; range, 20–70 s). The junction was 6 min $(379 \pm 53$ s) p.i., and 11 min p.i. was the minimum time when their SUV_{mean} value was similar to that at 60 min p.i. **D** Bone metastases' tracer uptake started very early (mean, 55 s; range, 20–70 s). The junction time was 8 min $(450 \pm 88$ s) p.i., and 35 min p.i. was the minimum time when their SUV_{mean} value was similar to that at 60 min p.i

Table 3 SUV_{mean} values of urinary bladder activity and pathologic lesions

	Urinary bladder	Prostate lesions	LN metastases	Bone metastases
Uptake pattern				
Initial uptake time	180 s	86 s (75–100 s)	35 s (20–70 s)	55 s (20–70 s)
Phase 1	Slow ascent (180–330 s)	Rapid increasing (initial uptake time–5 min)	Rapid increasing (initial uptake time–3.5 min)	Rapid increasing (initial uptake time–5 min)
Phase 2	Rapid ascent (330 s–60 min)	Slow ascent (5–60 min)	Slow ascent (3.5–60 min)	Slow ascent (5–60 min)
Junction point between urinary bladder activity and pathologic lesions				
Junction time	N/A	7.0 min (424 ± 19 s)	6.5 min (379 ± 53 s)	8.0 min (450 ± 88 s)
Comparing with the SUV_{mean} of corresponding lesions at 60 min p.i				
Lower	N/A	0–20 min	0–10.5 min	0–34 min
Equal	N/A	21–59 min	11–59 min	35–59 min

N/A not applicable

Representative ^{68}Ga-PSMA PET/CT images of a patient with prostate cancer acquired at 6 and 60 min p.i. for preoperative staging are shown in Fig. 5.

The tracer uptake by lymph node metastases started very early, increased rapidly during the first 3.5 min, and then slowly until the end of the dynamic study, reaching the highest SUV_{mean} at 60 min p.i. (Fig. 4C). The lymph node metastasis SUV_{mean} was higher than that of the urinary bladder activity between 35 and 360 s p.i.

Tracer uptake of bone metastases started very early, increased rapidly during the first 5 min, and then slowly and continuously until the end of the dynamic study, reaching the highest SUV_{mean} at 60 min p.i. (Fig. 4D). The SUV_{mean} of bone metastases was higher than that of the urinary bladder activity between 55 and 480 s p.i.

Comparison of the SUV$_{mean}$ values at 6, 35, 60, and 180 min p.i.

The junction times when the urinary bladder activity and the prostate lesions, lymph node metastases, or bone metastases had equal SUV_{mean} values were 7.0 min (424 ± 19 s), 6.5 min (379 ± 53 s), and 8.0 min (450 ± 88 s), respectively (Fig. 4 and Table 3). Therefore, the optimal time when the pathological lesion SUV_{mean} values were all lower than the urinary bladder activity but higher than all previous respective SUV_{mean} values was 6 min p.i. We further compared the pathological lesion SUV_{mean} values at 6 and 60 min p.i. (Fig. 6A) and found the values at 6 min p.i. to be lower for the prostate lesions (3.8 ± 0.6 vs. 8.0 ± 1.4, $P = 0.023$), lymph node metastases (2.0 ± 0.3 vs. 3.6 ± 0.5, $P = 0.011$), and bone metastases (3.9 ± 0.5 vs. 7.1 ± 1.1, $P = 0.001$).

The minimum time when the pathological lesion SUV_{mean} values were all similar to their corresponding SUV_{mean} values at 60 min p.i. was 35 min p.i. (Fig. 4 and Table 3; all $P > 0.05$). The prostate lesion SUV_{mean} at 180 min p.i. was higher than the corresponding values at 35 (13.6 ± 1.9 vs. 7.2 ± 1.2, $P = 0.013$) and 60 (13.6 ± 1.9 vs. 8.0 ± 1.4, $P = 0.035$) min p.i. (Fig. 6B). Similarly, the lymph node metastasis SUV_{mean} at 180 min p.i. was higher than the corresponding values at 35 (6.5 ± 1.0 vs. 3.3 ± 0.4, $P = 0.005$) and 60 (6.5 ± 1.0 vs. 3.6 ± 0.5, $P = 0.014$) min p.i. The bone metastasis SUV_{mean} at 180 min p.i. was higher than the corresponding values at 35 (12.7 ± 2.3 vs. 6.4 ± 1.0, $P = 0.015$) and 60 (12.7 ± 2.3 vs. 7.1 ± 1.1, $P = 0.032$) min p.i.

Of the eight prostate lesions visible on the ^{68}Ga-PSMA PET/CT maximum intensity projection (MIP; Fig. 6C), six (75.0%) were visible at 6 and 60 min p.i. The other two (25.0%) were not visible at 60 min p.i. due to urine interference. Six of the nine lymph node metastases visible on the ^{68}Ga-PSMA PET/CT MIP at 6 min p.i. were also visible at 60 min p.i. while the other three were obscured by urine interference. Of the 14 lymph node metastases visible on the MIP at 60 min p.i., eight (57.1%) were not visible at 6 min p.i. as their ^{68}Ga-PSMA uptake was low. Sixteen bone metastases were visible on the ^{68}Ga-PSMA PET/CT MIP at 6 and 60 min p.i. combined, of which six (37.5%) were visible in both. The three bone metastases (18.8%) visible at 6 but not 60 min p.i. were not visible due to urine interference, whereas the seven visible at 60 but not 6 min p.i. (43.7%) were not visible due to low ^{68}Ga-PSMA uptake. The numbers of prostate lesions, lymph node metastases, and bone metastases visible at 35 and 180 min p.i. were identical to those at 60 min p.i.

Fig. 5 ^{68}Ga-PSMA PET/CT of a patient with prostate cancer, performed for preoperative staging at 6 and 60 min p.i. **A** Maximum intensity projection (MIP) on ^{68}Ga-PSMA PET/CT at 6 min post-tracer injection (p.i.). Prostate lesions and left pubic, right iliac bone, and right acetabular metastases could be detected on the MIP, whereas the urinary bladder activity was not yet visible. **B** MIP on ^{68}Ga-PSMA PET/CT at 60 min p.i. The prostate lesions and left pubic metastasis could not easily be visualized due to the urinary bladder activity interference on the MIP. The right iliac bone and right acetabular metastases were visible on the MIP because the urine did not obscure them. **C** Fused axial PET/CT images at 6 min p.i. A red arrow points successively to the area of the prostate lesions and left pubic, right iliac bone, and right acetabular metastases. **D** The parallel fused axial PET/CT images at 60 min p.i. **E** Axial CT images of corresponding lesions
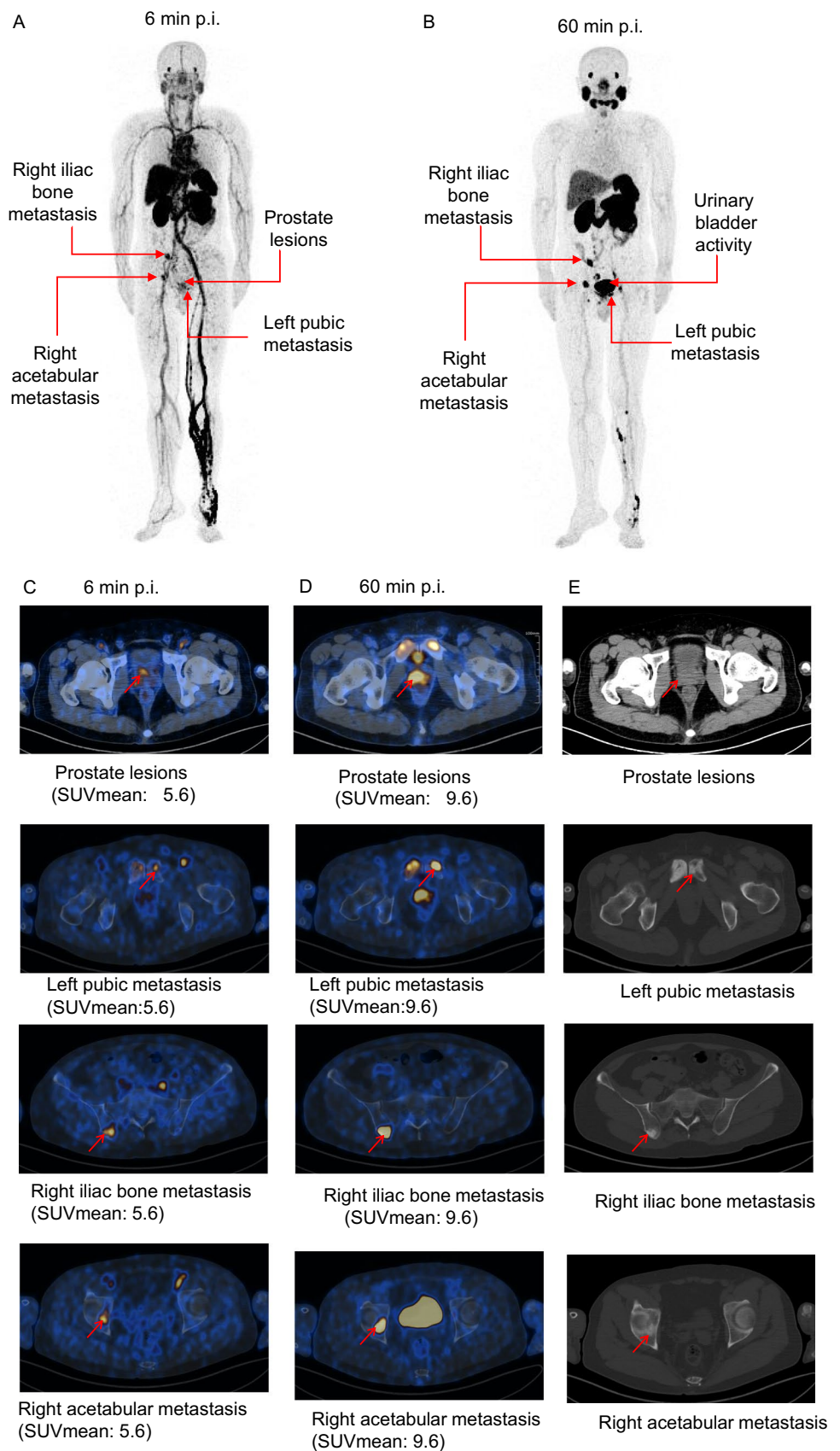
Fig. 6 A comparison of the SUV_{mean} at 6, 60, and 180 min p.i. ▶ **A** A comparison of pathological lesions SUV_{mean} values at 6 and 60 min post-tracer injection (p.i.). All SUV_{mean} values at 6 min p.i. were lower than the corresponding values at 60 min p.i.: prostate lesions, 3.8 ± 0.6 vs. 8.0 ± 1.4, $P=0.023$; lymph node (LN) metastases, 2.0 ± 0.3 vs. 3.6 ± 0.5, $P=0.011$; bone metastases, 3.9 ± 0.5 vs. 7.1 ± 1.1, $P=0.001$. **B** A comparison of pathological lesions SUV_{mean} at 180 min p.i. with the values at 35 and 60 min p.i. The prostate lesions, LN, and bone metastases SUV_{mean} values at 180 min p.i. were higher than the corresponding values at 35 and 60 min p.i. **C** The numbers of prostate lesions, LN metastases, and bone metastases visualized on ^{68}Ga-PSMA PET/CT MIP at 6 and 60 min p.i. Black columns represent the pathological lesions visible at 6 and 60 min p.i. Mixed columns represent the pathological lesions visible only at 6 min p.i. White columns represent the pathological lesions visible only at 60 min p.i

Discussion

We conducted a retrospective study to investigate the feasibility and potential benefits of whole-body dynamic ^{68}Ga-PSMA PET/CT acquisition in patients with prostate cancer.

Although static ^{68}Ga-PSMA PET/CT 60 min p.i. is recommended in clinical routine [3], small lesions such as local recurrences or lymph node metastases adjacent to the urinary bladder might be overlooked because of intense physiological urinary bladder uptake [3, 4]. And several methods such as administering diuretics or voiding the bladder before PET imaging did not reduce the urinary bladder activity sufficiently [5]. Therefore, we aimed to determine whether TB dynamic ^{68}Ga-PSMA PET in patients with prostate cancer could avoid the effect of urinary bladder activity when evaluating the lesions. Several studies [6] performed early dynamic ^{68}Ga-PSMA PET imaging during the first 8 min p.i., showing that it could differentiate pathological tracer uptake from physiological bladder activity. However, due to the limited AFOV of conventional PET scanners and relatively low sensitivity and signal-to-noise ratio, this dynamic imaging was limited to the pelvic region, and only early imaging was applied. Furthermore, previous dynamic images were acquired at a rate of 60 s per frame, which might be too slow to observe real-time changes in ^{68}Ga-PSMA uptake. To the best of our knowledge, this is the first study to assess normal organs and prostate cancer lesions by TB dynamic ^{68}Ga-PSMA PET.

Our study found that the primary prostate lesions, lymph node metastases, and bone metastases showed increased tracer uptake during the first 3 min p.i., when the urinary bladder activity was still not visible. The urinary bladder TAC showed a slow ascent between 180 and 330 s p.i. and a rapid increase after that, while uptake by the pathological lesions rapidly increased during the first 5 min and slowly increased until the end of the dynamic ^{68}Ga-PSMA PET. The pathological lesion SUV_{mean} values during the first
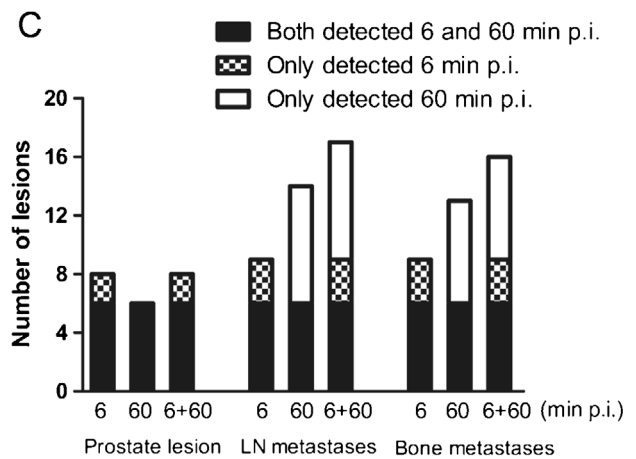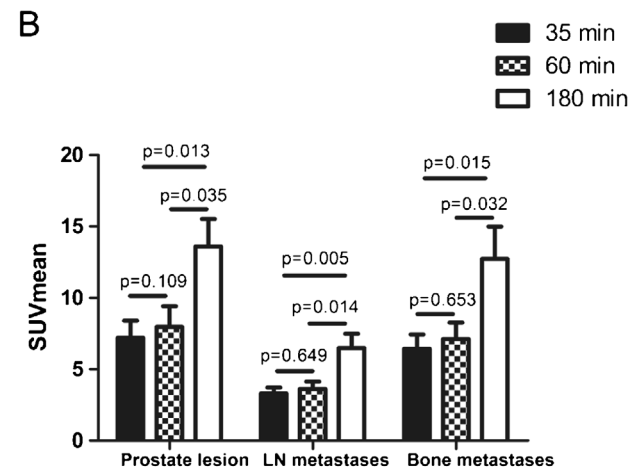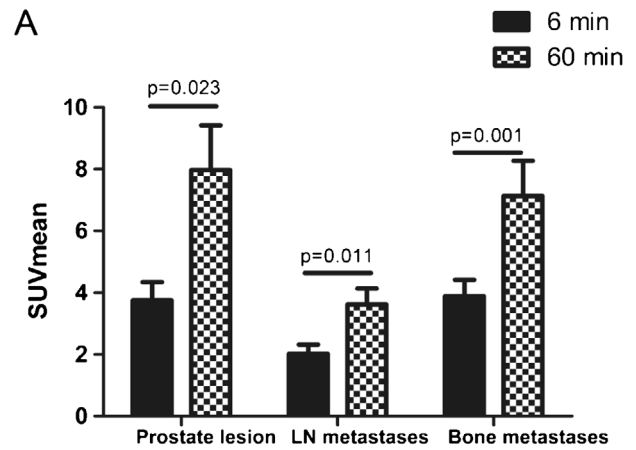
6 min p.i. were significantly higher than those in the urinary bladder. Therefore, pathological lesion evaluation by early dynamic ^{68}Ga-PSMA PET (75–360 s) could avoid the urinary bladder activity interference. A total of 25.0% of prostate lesions, 17.6% of the lymph node metastases, and 18.8% of the bone metastases could be observed at 6 min

p.i., which could not be easily observed at 60 min p.i. on the MIP due to urine interference. Consistent with our results, Kabasakal et al. [13] performed static [68] Ga-PSMA PET imaging for the pelvis 5 min p.i. in patients with prostate cancer and found it easier to assess prostate bed lesions on early PET/CT images than at 60 min p.i. because the bladder activity was absent. Barakat A et al. [14] [14] also found that the addition of early imaging significantly improved the overall detection rate of PSMA-avid lesions. However, the early SUV_{mean} values of the prostate lesions, lymph node metastases, and bone metastases were only one-third, one-half, and one-half of the corresponding values at 60 min p.i. A total of 57.1% of the lymph node metastases, and 43.7% of the bone metastases could not be easily detected on the MIP at 6 min p.i. due to their low [68] Ga-PSMA uptake. Pathological lesions with relatively low PSMA uptake might be missed if only early imaging were applied. A combination of early dynamic imaging during the first 6 min and static late imaging might better detect lesions obscured by the urinary bladder activity and those with relatively low PSMA uptake.

The pathological lesion PSMA uptake rose quickly during the first 5 min and then slowly until the end of the 60 min. We found that the pathological lesion SUV_{mean} values at 35–59 min p.i. and 60 min p.i. were similar, even though the SUV_{mean} values continuously increased. [68] Ga-PSMA PET/CT at 60 min p.i. is usually applied in clinical practice. Our study demonstrated that the range of 35 to 59 min p.i. was also acceptable for [68] Ga-PSMA PET/CT. The waiting time for examination could be reduced if [68] Ga-PSMA PET imaging was performed earlier than at 60 min p.i. We also performed delayed imaging (180 min p.i.), showing that the prostate lesion, lymph node, and bone metastasis SUV_{mean} values at 180 min p.i. were higher than the corresponding values at 35 and 60 min p.i. Delayed imaging (180 min p.i.) could be considered if conventional PET/CT imaging could not satisfy the clinical diagnosis.

We assess whole-body dynamic [68] Ga-PSMA PET for prostate cancer lesions and normal organs. The static [68] Ga-PSMA uptake characteristics of normal organs have been reported in many studies [12]; however, their dynamic uptake characteristics are still unknown. Our study found that the ascending aorta, cerebral cortex, and lung uptake rapidly increased and rapidly decreased; the liver, spleen, pancreas, bone, and muscle uptake rapidly increased and slowly decreased; the parotid gland, submandibular gland, and kidney uptake gradually increased. The PSMA is expressed on prostate cancer cells and many other malignant tumors [15–18]. Therefore, mastering the dynamic characteristics of PSMA uptake in normal organs could help better choose the time of PSMA imaging in non-prostate cancer tumors and select the appropriate normal reference organs at different imaging times.

Our study had several limitations. First, it was a retrospective study with a small sample. Moreover, although we found that pathological lesion SUV_{mean} values between 35 and 59 min p.i. were similar to the corresponding values at 60 min p.i., the SUV_{mean} values showed a continuous increase over this 60 min. So the small sample size may be underpowered to detect the difference if there were different pathological lesion SUV_{mean} values between 35 and 59 min and 60 min p.i. Prospective studies with more participants are needed to confirm our results. Furthermore, the lymph node and bone metastasis SUV_{mean} values at 180 min p.i. were higher than the corresponding values at 60 min p.i. Dynamic [68] Ga-PSMA PET of over 60 min might be necessary to find the [68] Ga-PSMA uptake plateau for the pathological lesions.

Conclusions

Our study demonstrated that early dynamic [68] Ga-PSMA PET/CT (75–360 s) evaluation of prostate cancer lesions could avoid the urinary bladder activity interference. However, the lower pathological lesions early SUV_{mean} values than at 60 min p.i. should be remembered. A combination of early dynamic imaging during the first 6 min and conventional static imaging 60 min p.i. might better detect lesions interfered by urinary bladder activity and those with relatively low PSMA uptake. The corresponding pathological lesion SUV_{mean} values between 35 and 59 min p.i. and at 60 min p.i. were similar (all $P > 0.05$), so [68] Ga-PSMA PET/CT imaging could also be made at other times in the range of 35–59 min p.i.

Declarations

Conflict of interest The authors declare no competing interests.

References

1. Perera M, Papa N, Roberts M, Williams M, Udovicich C, Vela I, Christidis D, Bolton D, Hofman MS, Lawrentschuk N, et al. Gallium-68 prostate-specific membrane antigen positron emission tomography in advanced prostate cancer-updated diagnostic utility, sensitivity, specificity, and distribution of prostate-specific membrane antigen-avid lesions: a systematic review and meta-analysis. Eur Urol. 2020;77(4):403–17.

2. Afshar-Oromieh A, Zechmann CM, Malcher A, Eder M, Eisenhut M, Linhart HG, Holland-Letz T, Hadaschik BA, Giesel FL, Debus J, et al. Comparison of PET imaging with a (68)Ga-LABELLED PSMA ligand and (18)F-choline-based PET/CT for the diagnosis of recurrent prostate cancer. Eur J Nucl Med Mol Imaging. 2014;41(1):11–20.

3. Fendler WP, Eiber M, Beheshti M, Bomanji J, Ceci F, Cho S, Giesel F, Haberkorn U, Hope TA, Kopka K *et al*: (68)Ga-PSMA PET/CT: Joint EANM and SNMMI Procedure Guideline for Prostate Cancer Imaging: Version 1.0. Eur J Nucl Med Mol Imaging 2017, 44(6):1014–1024.

4. Afshar-Oromieh A, Hetzheim H, Kubler W, Kratochwil C, Giesel FL, Hope TA, Eder M, Eisenhut M, Kopka K, Haberkorn U. Radiation dosimetry of (68)Ga-PSMA-11 (HBED-CC) and preliminary evaluation of optimal imaging timing. Eur J Nucl Med Mol Imaging. 2016;43(9):1611–20.

5. Afshar-Oromieh A, Malcher A, Eder M, Eisenhut M, Linhart HG, Hadaschik BA, Holland-Letz T, Giesel FL, Kratochwil C, Haufe S, et al. PET Imaging with a [68Ga]Gallium-labelled PSMA ligand for the diagnosis of prostate cancer: biodistribution in humans and first evaluation of tumour lesions. Eur J Nucl Med Mol Imaging. 2013;40(4):486–95.

6. Uprimny C, Kroiss AS, Decristoforo C, Fritz J, Warwitz B, Scarpa L, Roig LG, Kendler D, von Guggenberg E, Bektic J, et al. Early dynamic imaging in (68)Ga- PSMA-11 PET/CT allows discrimination of urinary bladder activity and prostate cancer lesions. Eur J Nucl Med Mol Imaging. 2017;44(5):765–75.

7. Badawi RD, Shi H, Hu P, Chen S, Xu T, Price PM, Ding Y, Spencer BA, Nardo L, Liu W, et al. First human imaging studies with the EXPLORER total-body PET scanner. J Nucl Med. 2019;60(3):299–303.

8. Zhang X, Zhou J, Cherry SR, Badawi RD, Qi J. Quantitative image reconstruction for total-body PET imaging using the 2-meter long EXPLORER scanner. Phys Med Biol. 2017;62(6):2465–85.

9. Cherry SR, Badawi RD, Karp JS, Moses WW, Price P, Jones T: Total-body imaging: transforming the role of positron emission tomography. Sci Transl Med 2017, 9(381).

10. Zhang X, Xie Z, Berg E, Judenhofer MS, Liu W, Xu T, Ding Y, Lv Y, Dong Y, Deng Z, et al. Total-body dynamic reconstruction and parametric imaging on the uEXPLORER. J Nucl Med. 2020;61(2):285–91.

11. Liu G, Xu H, Hu P, Tan H, Zhang Y, Yu H, Li X, Shi H. Kinetic metrics of (18)F-FDG in normal human organs identified by systematic dynamic total-body positron emission tomography. Eur J Nucl Med Mol Imaging. 2021;48(8):2363–72.

12. Demirci E, Sahin OE, Ocak M, Akovali B, Nematyazar J, Kabasakal L. Normal distribution pattern and physiological variants of 68Ga-PSMA-11 PET/CT imaging. Nucl Med Commun. 2016;37(11):1169–79.

13. Kabasakal L, Demirci E, Ocak M, Akyel R, Nematyazar J, Aygun A, Halac M, Talat Z, Araman A. Evaluation of PSMA PET/CT imaging using a 68Ga-HBED-CC ligand in patients with prostate cancer and the value of early pelvic imaging. Nucl Med Commun. 2015;36(6):582–7.

14. Barakat A, Yacoub B, Homsi ME, Saad Aldine A, El Hajj A, Haidar MB. Role of early PET/CT imaging with 68Ga-PSMA in staging and restaging of prostate cancer. Sci Rep. 2020;10(1):2705.

15. Kunikowska J, Cieslak B, Gierej B, Patkowski W, Kraj L, Kotulski M, Zieniewicz K, Krolicki L. [(68) Ga]Ga-prostate-specific membrane antigen PET/CT: a novel method for imaging patients with hepatocellular carcinoma. Eur J Nucl Med Mol Imaging. 2021;48(3):883–92.

16. Pozzessere C, Bassanelli M, Ceribelli A, Rasul S, Li S, Prior JO, Cicone F. Renal cell carcinoma: the oncologist asks, can PSMA PET/CT answer? Curr Urol Rep. 2019;20(11):68.

17. Raveenthiran S, Esler R, Yaxley J, Kyle S. The use of (68) Ga-PET/CT PSMA in the staging of primary and suspected recurrent renal cell carcinoma. Eur J Nucl Med Mol Imaging. 2019;46(11):2280–8.

18. Uijen MJM, Derks YHW, Merkx RIJ, Schilham MGM, Roosen J, Prive BM, van Lith SAM, van Herpen CML, Gotthardt M, Heskamp S et al: PSMA radioligand therapy for solid tumors other than prostate cancer: background, opportunities, challenges, and first clinical reports. Eur J Nucl Med Mol Imaging 2021.